Contribution from the Department of Chemistry,
York University, North York, Ontario, Canada M3J 1P3

Low-Spin Monoiron(III) and Oxo-Bridged Diiron(III) Complexes of Bis(difluoro(dimethylglyoximato)borate)

Dennis V. Stynes,* Horst Noglik, and David W. Thompson

Received April 9, 1991

New low-spin monomeric and oxo-dimeric complexes of $Fe^{III}N_4$[1] are described where N_4 is the tetradentate bis(difluoro(dimethylglyoximato)borate) macrocycle. Oxo-bridged species $[FeN_4(L)]_2O$ with labile axial ligands L = CH_3CN, pyridine (py), 1-methylimidazole (MeIm), or tosylmethyl isocyanide (TMIC) have low-energy oxo to Fe charge-transfer bands at 672, 690, 705, and 785 nm, respectively. Anions cleave the oxo bridge giving low-spin $Fe^{III}N_4X_2^-$ species (X = Cl^-, Br^-, NCS^-) with rhombic EPR spectra. Cyclic voltammetry and visible and EPR spectra are reported. The properties of this strong-field FeN_4 system are contrasted with weaker field systems such as Fe(salen) and hemes.

Introduction

The elucidation of the role of iron in living systems ultimately rests on a thorough knowledge of ligand-binding processes, electron transfer, and redox properties of its common oxidation states and how these properties depend upon the ligand environment around iron. We have previously reported extensive rate and equilibria[2-5] measurements of axial ligand substitution processes for a series of low-spin ferrous bis(dioximate) complexes and here extend these studies to ferric derivatives.

Studies of high-spin ferric systems including Fe(salen)[6-8] and a variety of oxo-bridged complexes[9] have helped elucidate the role of Fe(III) in such enzymes as uteroferrin, hemerythrin, catechol 1,2-dioxygenase,[10] and purple acid phosphatases.[11]

We report here the synthesis and some reactions of strongly oxidizing Fe(III) complexes of the oxidatively stable, acid resistant $(dmgBF_2)_2$ (abbreviated as N_4 throughout) ligand in which the strong-field N_4 donor set confers a low-spin state on the complexes. This system provides one of the few examples of low-spin ferric complexes which could serve as bioinorganic models for hemes, bleomycin,[12-14] and an emerging class of low-spin non-heme iron proteins such as nitrile hydratase.[15,16]

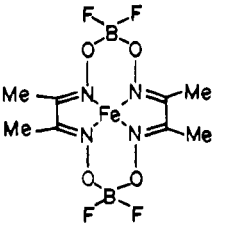

FeN_4

Experimental Section

Materials. The complex $FeN_4(CH_3CN)_2$ was synthesized as described previously.[2] Other materials were commercially available and used as received.

Physical Measurements. Visible spectra of solutions (typically in 1 cm path length cells) were recorded on an Aminco DW-2a UV/vis spectrophotometer. Infrared spectra of samples as KBr disks were obtained on a Nicolet 20 SX FTIR instrument. Elemental analyses were performed by Canadian Microanalytical Service Ltd., Vancouver, BC, Canada.

EPR spectra were obtained on a Varian E4 spectrometer (ν = 9.250 GHz) in frozen-CH_3CN solutions at 110 K. Concentrations of complexes were routinely 10^{-4} M.

Cyclic voltammetry experiments, referenced to SCE, were performed on solutions in dry CH_3CN with 0.1 M TEAP as supporting electrolyte using a PAR electrochemical apparatus as described previously.[2] Reversibility was examined on the basis of anodic to cathodic peak current ratios of unity, linear plots of peak current vs the square root of the scan rate, and peak separations typically between 60 and 90 mV for scan rates between 20 and 500 mV s^{-1}.

Syntheses. $[FeN_4(CH_3CN)]_2O$. The $FeN_4(CH_3CN)_2$ complex (1 g, 2.2 mol) was stirred in 120 mL of acetone in air for 3 h. The solution was filtered, and the filtrate was added to 300 mL of hexane giving a dark green precipitate. The solid was washed with CH_3CN to remove unreacted starting material and dried in vacuo. Yield: 0.56 g (59%). Anal. Calcd for $Fe_2C_{20}H_{30}B_4F_8N_{10}O_9$: C, 27.9; H, 3.5; N, 16.3. Found: C, 27.9; H, 3.4; N, 16.1. Visible: CH_3CN, ϵ = 10600 M^{-1} cm^{-1} at λ_{max} = 672 nm; CH_2Cl_2, ϵ = 19300 M^{-1} cm^{-1} at λ_{max} = 392 nm.

$[FeN_4(L)]_2O$. The $FeN_4(CH_3CN)_2$ complex was oxidized in acetone as described above and filtered to remove insolubles, and an excess of ligand L was added (L = py, MeIm, TMIC). Addition of hexane induced precipitation. The isolated solids were washed with a small amount of CH_3CN containing L, followed by diethyl ether.

$Et_4N[FeN_4Cl_2]$. The $FeN_4(CH_3CN)_2$ complex (0.7 g, 1.5 mmol) was oxidized in 90 mL of rapidly stirred acetone in air over 1 h and filtered to remove insolubles, and then (TEA)Cl (0.47 g, 2.9 mmol) was added. The solution was stirred for 30 min, and the volume was reduced to give a dark solid. The product was filtered off, recrystallized from acetone containing (TEA)Cl, and dried in vacuo. Yield: 0.4 g. Anal. Calcd for $FeC_{16}H_{32}B_2Cl_2F_4N_5O_4$: C, 32.97; H, 5.66; N, 12.01; Cl, 12.16. Found: C, 33.2; H, 5.3; N, 11.9; Cl, 12.4. IR (KBr): 1608 ($\nu_{C=N}$, $dmgBF_2$), 384 cm^{-1} (ν_{Fe-Cl}). Visible: ϵ = 5240 M^{-1} cm^{-1} at λ_{max} = 423 nm.

$Et_4N[FeN_4Br_2]$ was obtained by an analogous method. Yield: 63%. IR (KBr): 1601 ($\nu_{C=N}$, $dmgBF_2$), 333 cm^{-1} (ν_{Fe-Br}).

In Situ Generation of Complexes. $FeN_4(CH_3CN)_2^+$. Solutions of $FeN_4Cl_2^-$ were treated with 2 equiv of $AgPF_6$, and the AgCl was removed by centrifugation. Solutions with identical spectra (visible and EPR) could also be generated by controlled-potential electrolysis of $FeN_4(CH_3CN)_2$ solutions or careful addition of $HClO_4$ or H_2SO_4 to solutions

(1) Abbreviations: The bis(difluoro(dimethylglyoximato)borate) ligand is N_4 throughout. Other abbreviations are as follows: py, pyridine; MeIm, 1-methylimidazole; TMIC, (*p*-tolylsulfonyl)methyl isocyanide; TEAP, (TEA)Cl, and (TEA)Br are tetraethylammonium perchlorate, chloride, and bromide, respectively; salen, 1,2-bis(salicylideneamino)ethanato(2-); tim, 2,3,9,10-tetramethyl-1,2,8,11-tetraazacyclotetradeca-1,3,8,10-tetraene; Pc, phthalocyanine; tpp, tetraphenylporphyrin; PPIXDME, protoheme-IX dimethyl ester; diaammac, 6,13-dimethyl-1,4,8,11-tetraazacyclotetradecane-6,13-diamine; BLM, bleomycin; bpy, bipyridine; H_2Q, hydroquinone; Q, quinone; tmpd, *N,N,N',N'*-tetramethyl-1,4-phenylenediamine; LMCT, ligand to metal charge transfer; MLCT, metal to ligand charge transfer.

(2) Stynes, D. V.; Thompson, D. W. *Inorg. Chem.* **1990**, *29*, 3815.
(3) Stynes, D. V.; Thompson, D. W. *Inorg. Chem.* **1991**, *30*, 636.
(4) Chen, X. C.; Stynes, D. V. *Inorg. Chem.* **1986**, *25*, 1173.
(5) Stynes, D. V. *Pure Appl. Chem.* **1988**, *561*, 60.
(6) Que, L., Jr. *Coord. Chem. Rev.* **1983**, *50*, 73.
(7) Que, L., Jr.; Lauffer, R. B.; Lynch, J. B.; Murch, B. P.; Pyrz, J. W. *J. Am. Chem. Soc.* **1987**, *109*, 5381.
(8) Pyrz, J. W.; Roe, A. L.; Stern, L. J.; Que, L., Jr. *J. Am. Chem. Soc.* **1985**, *107*, 614.
(9) Kurtz, D. M. *Chem. Rev.* **1990**, *90*, 585.
(10) Lauffer, R. B.; Heistand, R. H.; Que, L., Jr. *Inorg. Chem.* **1983**, *22*, 50.
(11) Vincent, J. B.; Olivier-Lilley, G. L.; Averill, B. A. *Chem. Rev.* **1990**, *90*, 1447.
(12) Suguira, Y. *J. Am. Chem. Soc.* **1980**, *102*, 5208.
(13) Lomis, T. J.; Elliot, M. G.; Siddiqui, S.; Moyer, M.; Koepsel, R. R.; Shepherd, R. E. *Inorg. Chem.* **1989**, *28*, 2369.
(14) Stubbe, J.; Kozarich, J. W. *Chem. Rev.* **1987**, *87*, 1107.
(15) (a) Sugiura, Y.; Kuwahara, J.; Nagasawa, H.; Yamada, H. *J. Am. Chem. Soc.* **1987**, *109*, 5848. (b) Sakuria, H.; Migita, K.; Tsuchiya, K. *Inorg. Chem.* **1988**, *27*, 1377. (c) Van Atta, R. B.; Long, E. C.; Hecht, S. M.; van der Marel, G. A., van Boom, J. H. *J. Am. Chem. Soc.* **1989**, *111*, 2722.
(16) Other references to low-spin Fe(III) macrocycles include: (a) Maroney, M. J.; Baldwin, D. A.; Stenkamp, R. E.; Jensen, L. H.; Rose, N. J. *Inorg. Chem.* **1986**, *25*, 1409. (b) Bernhardt, P.; Comba, P.; Hambley, T. W.; Lawrence, G. A. *Inorg. Chem.* **1991**, *30*, 942. (c) Dabrowiak, J. C.; Busch, D. H. *Inorg. Chem.* **1975**, *14*, 1881. (d) Goedken, V.; Busch, D. H. *J. Am. Chem. Soc.* **1972**, *94*, 3397. (e) Koch, S.; Holm, R. H.; Frankel, R. B. *J. Am. Chem. Soc.* **1975**, *97*, 6714.

0020-1669/91/1330-4567$02.50/0

Table I. Visible Spectral Data

complex	λ_{max}, nm (log ϵ)
Oxo-bridged Complexes	
$[FeN_4(CH_3CN)]_2O$	672 (4.03), sh 860, 446
$[FeN_4(MeIm)]_2O$	688 (4.06), sh 810, 524
$[FeN_4(py)]_2O$	708 (4.06), sh 850, 507
$[FeN_4(TMIC)]_2O$	781 (4.15), sh 650, 430
$[FeN_4]_2O$	392 (4.29)
$[Ru(bpy)_2Cl]_2O$[a]	672 (4.25)
$[Ru(bpy)_2NO_2]_2O$[a]	632 (4.41)
Monomeric Complexes	
$FeN_4(CH_3CN)_2^+$	409 (3.48), sh 390
$FeN_4Cl_2^-$	423 (3.72), 357
$FeN_4Br_2^-$	500 (3.28), 438 (3.64)
$FeN_4(SCN)_2^-$	626 (3.89), 413 (bd)

[a] Reference 26.

of the $[FeN_4(CH_3CN)]_2O$ complex. (Excess strong acids resulted in decomposition.)

Results

Synthesis and Characterization. Aerobic oxidation of the weak donor complex $FeN_4(CH_3CN)_2$ in poor donor solvents like acetone or dichloromethane (no reaction occurs in CH_3CN in air) results in the rapid formation of a species assigned to a μ-oxo-bridged diiron complex (eq 1). The oxo-bridged complex is characterized

$$2FeN_4(CH_3CN)_2 + \tfrac{1}{2}O_2 \rightarrow [FeN_4(CH_3CN)]_2O \quad (1)$$

in CH_3CN solution by its lack of an EPR signal, characteristic visible band at 672 nm, and stoichiometric reduction by hydroquinone (eq 2) or tmpd (*N,N,N',N'*-tetramethylphenylenediamine)

$$[FeN_4(CH_3CN)]_2O + H_2Q \rightarrow 2FeN_4(CH_3CN)_2 + Q + H_2O \quad (2)$$

$$[FeN_4(CH_3CN)]_2O + 2tmpd \rightarrow 2FeN_4(CH_3CN)_2 + 2tmpd^{\bullet+} \quad (3)$$

(eq 3).[17,18] The observed stoichiometry rules out a peroxo-bridged dimer analogous to that reported in the reaction of a triphenylphosphine oxide complex of Fe(II) with peroxides.[19] The oxo-bridged complex undergoes a variety of reactions including axial ligation, oxo-bridge cleavage with anions or acids, and reduction to well-defined Fe(II) complexes.

Treatment of the $[FeN_4(CH_3CN)]_2O$ complex in CH_3CN solution with acids (perchloric, sulfuric, acetic) or anions (chloride, bromide, thiocyanate) bleaches the low-energy LMCT band, giving solutions displaying rhombic EPR signals typical of low-spin monomeric Fe(III) complexes.[20,21] These species are distinct from the oxo dimers in lacking the low-energy oxo to metal CT band and giving only weaker bands in the 400-nm region.

The monomeric $FeN_4Cl_2^-$ complex was prepared via reaction 4 and gave an elemental analysis, rhombic EPR signal, and the

$$[FeN_4(CH_3CN)]_2O + 4Cl^- \rightarrow 2FeN_4(Cl)_2^- \quad (4)$$

Fe–Cl stretch at 384 cm^{-1} in the IR fully consistent with the proposed formulation. The stoichiometric reduction of the complex with tmpd (eq 5) and titration with $AgPF_6$ (eq 6) corroborate the structure in solution.

$$FeN_4Cl_2^- + tmpd \rightarrow FeN_4(CH_3CN)_2 + tmpd^{\bullet+} + 2Cl^- \quad (5)$$

$$FeN_4Cl_2^- + 2Ag^+ \rightarrow FeN_4(CH_3CN)_2^+ + 2AgCl(s) \quad (6)$$

Spectral Features. The visible spectra for the oxo-bridged diiron and monomeric complexes are given in Table I. The visible spectrum of the $[FeN_4(CH_3CN)]_2O$ complex is dominated by an intense band at 672 nm assigned to oxo to Fe charge transfer with weaker bands around 440 nm assigned to oxime to Fe charge transfer. The oxo–iron CT band shifts on adding ligands, consistent with the axial ligation reaction

$$[FeN_4(CH_3CN)]_2O + 2L \rightarrow [FeN_4(L)]_2O + 2CH_3CN \quad (7)$$

The LMCT band shifts, as expected, to lower energy for π-acceptor ligands (TMIC) in contrast to the opposite trends found for MLCT bands in Fe(II) complexes.[3]

Solutions of the oxo-bridged complex in noncoordinating solvents (CH_2Cl_2) lack the low-energy band at 672 nm but show a new band at 392 nm typical of many high-spin oxo-bridged species.[9] The "392" species is proposed to be an unligated high-spin oxo-bridged diiron species, as it lacks an EPR spectrum, behaves chemically like an oxo-bridged species, and converts to "672" on addition of CH_3CN. The shift in the visible band assigned to oxo to iron CT is attributed to spin-pairing energy considerations for low- vs high-spin Fe(III).[22] The difference in the spin-pairing energy (SPE) for t_{2g}^5 ($^{14}/_3B$) vs $t_{2g}^3e_g^2$ ($^{56}/_3B$) corresponds exactly to the difference in the charge-transfer band energies (10630 cm^{-1}) if a Racah B value for Fe(III) of 760 cm^{-1} is used. Carrano has described a similar effect in tyrosine to iron CT bands of low- and high-spin Fe(III).[23]

Monomeric ferric derivatives lack the low-energy oxo band and give higher energy features associated with LMCT bands due to charge transfer from axial ligands Cl^-, Br^-, and NCS^-. A plot of these band positions vs optical electronegativity parameters[22,24] for the ligands gives a straight line fitting the equation

$$\nu_{CT} = 19.17X_L - 33.82 = 19.17(X_L - X_M) + \Delta SPE \quad (8)$$

where X_L and X_M are the optical electronegativities for the ligand and metal, respectively, and ΔSPE is the spin-pairing energy, which for the t_{2g}^5 case here is $^{14}/_3B$.[22] Using a value of B = 760 cm^{-1}, we calculate X_M to be 2.0.

The visible spectroscopy of the FeN_4 system bears a striking resemblance to an analogous ruthenium $Ru(bpy)_2$ system described by Meyer.[26] The M(II) complexes show intense MLCT bands, the M(III) oxo dimers have lower energy oxo to metal CT bands (ϵ = (10–20) × 10^3 M^{-1}/cm^{-1}), and monomeric M(III) derivatives give rise to somewhat weaker LMCT bands at higher energies than oxo to metal CT bands. These spectroscopic similarities are a result of both systems being low spin and lying at similar M(II,III) potentials.

EPR. The monomeric low-spin Fe(III) complexes display characteristic rhombic **g** tensors whose principal g values are extremely sensitive to the nature of the axial ligands. Analysis of the three g values according to established theory for low-spin d^5[16b,20] provides the axial (μ/λ) and rhombic (Δ/λ) crystal field distortion parameters in units of the spin–orbit coupling constant λ. Since the EPR experiment does not provide information about the labeling (x, y, z) and signs of the g values, we have examined all 48 possible combinations. From the few which satisfy the normalization criterion, we have selected a single solution which has a positive value of the rhombic distortion parameter and

(17) The titration requires the presence of Cl^-.[34]
(18) Michaelis, L.; Schubert, M. P.; Granick, S. *J. Am. Chem. Soc.* **1939**, *61*, 1981.
(19) Sawyer, D. T.; McDowell, M. S.; Spencer, L.; Tsang, P. K. J. *Inorg. Chem.* **1989**, *28*, 1166.
(20) Wave functions used for the ground-state Kramer's doublet follow the treatment of: Bohan, T. L. *J. Magn. Reson.* **1977**, *26*, 109. $|1+\rangle = A|1+\rangle + {}^1/_2B[\sqrt{2}(|2-\rangle - |-2-\rangle)] + C|-1+\rangle$; $|1-\rangle = -A|-1-\rangle + {}^1/_2B[\sqrt{2}(|2+\rangle - |-2+\rangle)] - C|-1-\rangle$.
(21) (a) Gadsby, P. M. A.; Thomson, A. J. *J. Am. Chem. Soc.* **1990**, *112*, 5003. (b) Taylor, C. P. S. *Biochim. Biophys. Acta* **1977**, *491*, 137.
(22) Lever, A. B. P. *Inorganic Electronic Spectroscopy*, 2nd ed., Elsevier: Amsterdam, 1984; pp 218–223.
(23) Spatalian, K.; Carrano, C. J. *Inorg. Chem.* **1989**, *28*, 19.
(24) X_L values used were as follows: Cl^-, 3.0; Br^-, 2.8; SCN^-, 2.6.
(25) As these parameters are based on systems of quite different redox potential in aqueous solution, we do not attach any significance to the derived parameters. The observed correlation is presented here merely as support for the LMCT assignments.
(26) Weaver, T. R.; Meyer, T. J.; Adeyemi, S. A.; Brown, G. M.; Eckberg, R. P.; Hatfield, W. E.; Johnson, E. C.; Murray, R. W.; Unterecker, D. *J. Am. Chem. Soc.* **1975**, *97*, 3039.

Table II. EPR Data, MO Coefficients, and Distortion Parameters for Fe(III) Complexes

complex	g_1	g_2	g_3	assgnt	A	B	C	μ/λ	Δ/λ
$FeN_4(CH_3CN)_2^+$	2.329	2.219	1.959	(x, y, z)	0.098	0.999	−0.017	−7.91	2.96
$FeN_4Ci_2^-$	2.341	2.191	1.962	(x, y, z)	0.095	0.999	−0.023	−8.44	4.44
$FeN_4Br_2^-$	2.380	2.238	1.953	(x, y, z)	0.109	1.000	−0.022	−7.23	3.11
Fe(diammac)[a]	2.841	2.463	1.631	(x, y, z)	0.266	0.978	−0.049	−3.03	1.38
$Fe(Ph_2[14]N_4)Br(dmf)$[b]	2.09	2.06	1.99	*c*					
nitrile hydratase[d]									
native R312	2.284	2.140	1.971	(x, y, z)	0.077	0.999	−0.023	−10.62	6.68
nitrile bound[e]	2.230	2.163	1.982	(x, y, z)	0.069	1.000	−0.011	−10.97	3.60
bleomycin[f]									
Fe(BLM)(OH_2)	2.254	2.171	1.937	(x, y, z)	0.087	0.992	−0.013	−8.68	2.79
Fe(BLM)(OH)	2.431	2.185	1.893	(x, y, z)	0.126	0.989	−0.037	−6.60	4.26
Fe(BLM)(C_6H_5OH)	2.423	2.187	1.895	(x, y, z)	0.124	0.989	−0.036	−6.08	2.48
$Fe(PPIXDME)(MeIm)_2^+$[g]	2.90	2.29	1.57	$(-z, x, -y)$	0.857	0.134	−0.507	3.38	2.02

[a] Reference 16b. [b] Reference 16c. [c] g-tensor anisotropy too small to give reliable results. [d] Reference 15a. [e] Nitrile bound is propionitrile. [f] Reference 12. [g] Tang, S. C.; Koch, S.; Papaefthymiou, G. C.; Foner, S.; Frankel, R. B.; Ibers, J. A.; Holm, R. H. *J. Am. Chem. Soc.* **1976**, *98*, 2414.

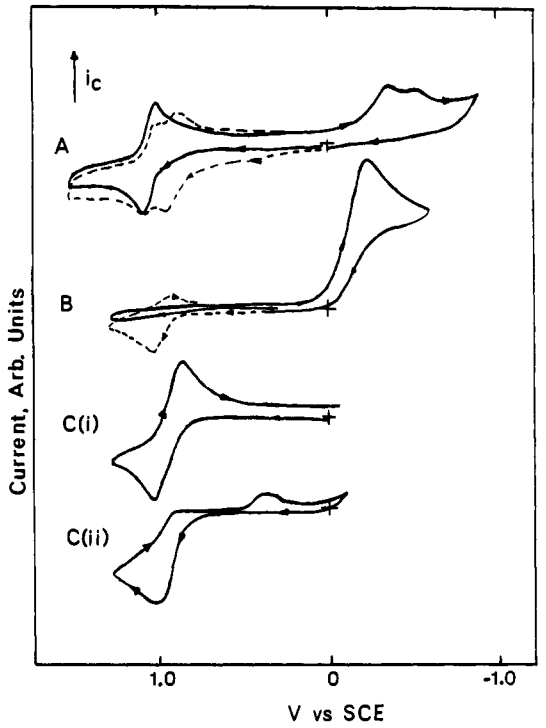

Figure 1. Cyclic voltammograms in CH_3CN ([TEAP] = 0.1 M) at 200 mV/s^{-1} scan rates (dashed lines show subsequent scans): (A) $[FeN_4(CH_3CN)]_2$ (0.4 mM); (B) $[FeN_4Cl_2^-]$ (2.0 mM); (C) $FeN_4(CH_3CN)_2$ (1.3 mM), (i) $[Cl^-]$ = 0 mM and (ii) $[Cl^-]$ = 1.3 mM.

maximizes the absolute value of the axial distortion parameter. This result is given in Table II along with our analysis of data for other systems.[21] Analyses of EPR results reported for nitrile hydratase and some bleomycin systems are seen to be quite similar to those for FeN_4 and are generally consistent with a $(d_{xz,yz})^4(d_{xy})^1$ ground state. Heme systems, however, typically have the hole in d_{yz}.[21]

For the $FeN_4Br_2^-$ ion, a seven-line hyperfine structure on g_3 is observed (a_{Br} = 21/G) consistent with that expected for coupling with two Br^- ($I = {}^3/_2$).[27] The detection of Br hyperfine coupling only on g_3 is consistent with the assignment $g_3 = g_z$ based on the analysis above.

Electrochemistry. Cyclic voltammetry results for $[FeN_4(CH_3CN)]_2O$ and some monomeric derivatives with anionic ligands are shown in Figure 1, and the data are collected along with previous results obtained with Fe(II) derivatives in Table III.

Table III. Electrochemical Data in Acetonitrile Solution

complex	E, V vs SCE (ΔE_p, mV) $E_{1/2}(Fe^{III/II})$	$E_{1/2}^{oxidn}$	ref
Oxo-Bridged Complexes			
$[FeN_4(CH_3CN)]_2O$	−0.40[b]	1.08 (80)	this work
$[FeN_4(MeIm)]_2O$	−0.75[b]	0.85 (130)	this work
$[Fe(TPP)]_2O$	−1.03		29
$[Fe(Pc)]_2O$	−0.59	0.47	29
$[Fe(Ph_2)[16]N_4]_2O$	−1.19		31
$[Fe(salen)]_2O$	−1.05		30
$[Ru(bpy)_2Cl]_2O$	−0.32	0.68	26
$[Ru(bpy)_2NO_2]_2O$	−0.15	0.94	26
Monomeric Complexes			
$FeN_4(CH_3CN)_2$	0.95 (85)		2
$FeN_4(py)_2$	0.76		2
$FeN_4(MeIm)_2$	0.46		2
$FeN_4(CH_3CN)CN^-$[c]	0.48 (100)		this work
$FeN_4(py)CN^-$	0.44 (100)		this work
$FeN_4(MeIm)CN^-$	0.32 (200)		this work
$FeN_4(CH_3CN)Cl^-$	0.35 (irr)[b]		this work
$FeN_4(Cl)_2^-$	−0.35 (irr)[b]		this work
Fe(TPP)F	−0.57		29b
Fe(TPP)Cl	−0.29		
Fe(TPP)Br	−0.21		
$Fe(salen)(CH_3CN)_2^+$	−0.35		40
Fe(salen)F	−0.76		
Fe(salen)Cl	−0.35		
Fe(salen)CN	−0.22		
Fe(BLM)	−0.15		15c

[a] Assigned to a metal-centered one-electron oxidation; see text for details. [b] Irreversible, cathodic potential reported. [c] Irreversible when CN^- is in excess.

The CV for $FeN_4(CH_3CN)]_2O$ in CH_3CN is shown in Figure 1A. A quasi-reversible wave at 1.08 V vs SCE is assigned to a metal-centered oxidation producing a mixed-valent species:

$$[FeN_4(CH_3CN)]_2O \rightarrow [FeN_4(CH_3CN)]_2O^+ + e^- \quad (9)$$

Analogous one-electron oxidations have been observed in [Fe(phthalocyanine)py]$_2O$[29] and $[Ru(bpy)_2Cl]_2O$[26] systems. Results for $[FeN_4(MeIm)]_2O$ show the expected dependence of the oxidation on the axial ligand trans to the oxo bridge.

If the sample is scanned cathodically from 0 V, two irreversible reduction waves are observed. The potential of the first process depends upon scan rate, shifting cathodically 50 mV per decade of sweep rate, indicative of a rapid chemical reaction following

(27) Br has two isotopes in approximately equal abundance with $I = {}^3/_2$. To our knowledge, this is the first observation of Br hyperfine coupling in a low-spin Fe complex.

(28) Kadish, K. M.; Larson, G.; Lexa, D.; Momenteau, M. *J. Am. Chem. Soc.* **1975**, *97*, 282.

(29) Bottomley, L. A.; Ercolani, C.; Gorce, J. N.; Pennesi, G.; Rossi, G. *Inorg. Chem.* **1986**, *25*, 2339.

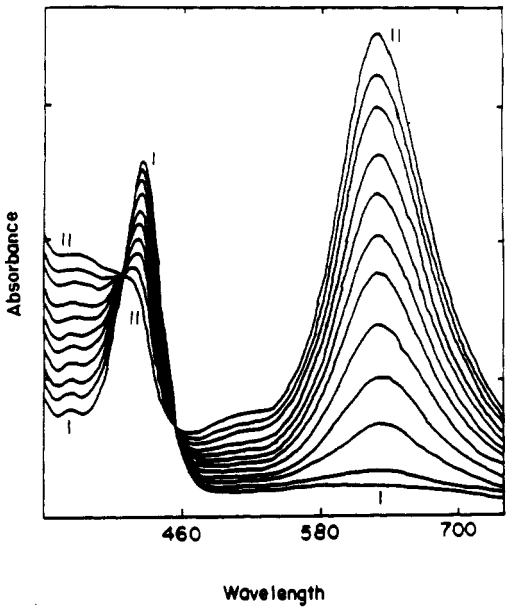

Figure 2. Spectral changes with time for the reaction of $FeN_4Cl_2^-$ + SCN^- ($[FeN_4Cl_2^-]$ = 0.3 mM; $[SCN^-]$ = 0.005 M) in CH_3CN. For increasing absorbances at 626 nm, times are 0, 10, 20, 33, 48, 61, 78, 97, 130, 162, and 228 min, respectively.

the charge-transfer process. This behavior is consistent with the reduction of the oxo-bridged species (eq 10) followed by oxo-bridge

$$[FeN_4(CH_3CN)]_2O + e^- \rightarrow [FeN_4(CH_3CN)]_2O^- \quad (10)$$

$$[FeN_4(CH_3CN)]_2O^- \rightarrow FeN_4(CH_3CN)_2 + FeN_4O^- \quad (11)$$

cleavage (eq 11), giving $FeN_4(CH_3CN)_2$ (seen to be oxidized at 0.95 V on the subsequent scan) and another species tentatively assigned to $[FeN_4O]^-$, which is reduced at −0.55 V.

Similar irreversible electrochemistry has been observed in $[Fe(phthalocyanine)py]_2O$[29] and $[Fe(salen)]_2O$[30] systems. The relative stability of the oxo bridge in the oxidized and reduced species is in agreement with MO considerations previously advanced by Meyer[26] and Bottomley.[29] Oxidation involves removal of an electron which is antibonding with respect to the Fe–O–Fe linkage.

Monomeric species display reversible to quasi-reversible waves assigned to the Fe(II/III) couple unless a ligand-exchange process complicates the CV experiment as for the chloride case shown in Figure 1B.

The CV scan for CH_3CN solutions of $FeN_4Cl_2^-$ gives a cathodic wave E_{pc} = −0.35 V with no return wave consistent with rapid dissociation of Cl^- upon reduction to Fe(II). CV waves for solutions of $FeN_4(CH_3CN)_2$ in CH_3CN are altered on addition of low $[Cl^-]$ consistent with an ECE mechanism involving rapid Cl^- trapping of the oxidation product

$$FeN_4(CH_3CN)_2^+ + Cl^- \rightarrow FeN_4(CH_3CN)Cl + CH_3CN \quad (12)$$

followed by electrochemical reduction of $FeN_4(CH_3CN)Cl$ at 0.35 V and subsequent dissociation of Cl^- from the Fe(II) species to regenerate $FeN_4(CH_3CN)_2$. Independent experiments give binding constants and rate constants for Fe(II) (K_{Cl} = 25 M^{-1} and k_{Cl} = 100 s^{-1})[32] fully consistent with these observations.

Reactions. A variety of reactions of the ferric species were surveyed, and they are summarized below.

Ligand-substitution reactions of $FeN_4Cl_2^-$ with Br^- and SCN^- (Figure 2) proceed with clean isosbestic points at a rate (2×10^{-4} s^{-1}) independent of the concentration or nature of the entering ligand indicative of a D mechanism for ligand substitution. No

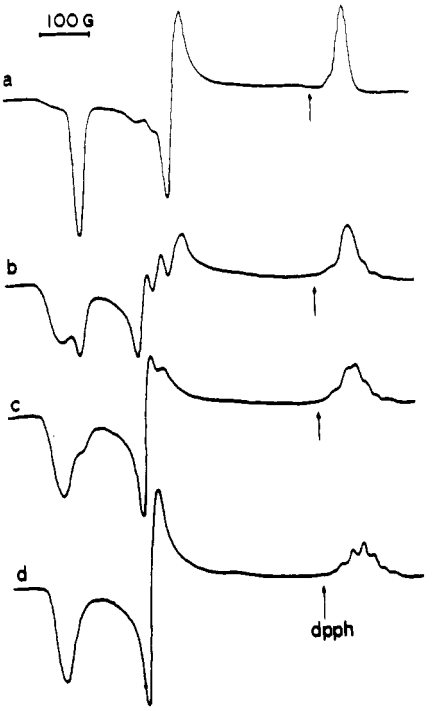

Figure 3. EPR spectra during the reaction $FeN_4Cl_2^-$ + $2Br^-$ = $FeN_4Br_2^-$ + $2Cl^-$ ($[Br^-]$ = 1.0 M) at room temperature. Spectra a–d were collected over a period of 2 h periodically by freezing the reaction solution to 110 K.

definitive evidence for mixed-ligand species was found by monitoring the reactions by visible or EPR spectroscopy (Figure 3). Reactions with MeIm or py also proceed at a similar rate limited by Cl^- dissociation; however, in these cases spontaneous reduction to FeN_4L_2 occurs with no evidence for Fe(III) species coordinated with MeIm. k_{-Cl} for $FeN_4Cl_2^-$ in CH_3CN is 6 orders of magnitude slower than that found in the $FeN_4(CH_3CN)Cl^-$ complex.[32]

Reduction of $FeN_4Cl_2^-$ with the presumably inner-sphere reductant hydroquinone is relatively slow compared to the much more rapid reaction with Wurster's reagent, which gives the readily identified blue radical[18] and $FeN_4(CH_3CN)_2$ in a stoichiometric reaction. However, if the bound chlorides are removed by treatment with Ag^+, a very labile Fe(III) species assigned as the $FeN_4(CH_3CN)_2^+$ ion is formed, which reacts rapidly in substitution and redox reactions. A dramatic example comes in the reaction with stoichiometric amounts of CN^-, which results in rapid reduction to $FeN_4(CH_3CN)_2$.[33]

Reactions of the oxo-bridged species give ligation trans to the oxo bridge with MeIm, py, and TMIC and slow reduction to Fe(II) complexes with quinones, phosphines, phenols, and other reducing agents. The oxo-bridged complex is generally a poorer oxidant both kinetically and thermodynamically than monomeric ferric species. Detailed kinetic investigations of these reactions will be reported elsewhere.[34]

Discussion

Two very important features of the FeN_4 system account for the distinctive chemistry of this system compared to a variety of other ferric complexes described in the literature.

First, the ability of the strong-field N_4 ligand to confer a low-spin electronic structure on the iron even for the weakest of axial ligands (Cl^-, oxo, CH_3CN, etc.) leads to much more inert complexes and results in apparently exclusively six-coordination. In contrast Fe(salen) complexes[35] are typically high spin, penta-

(30) Wenk, S. E.; Schultz, F. A. *J. Electroanal. Chem. Interfacial Electrochem.* **1979**, *101*, 89.
(31) Koch, S.; Holm, R. H.; Frankel, R. B. *J. Am. Chem. Soc.* **1975**, *97*, 6714.
(32) de Silva, H.; Thompson, D. W.; Stynes, D. V. *Inorg. Chem.*, in press.
(33) At greater than 1 equiv of CN^-, $FeN_4(CH_3CN)CN^-$ is the observed product absorbing at 490 nm.
(34) Noglik, H.; Thompson, D. W.; Stynes, D. V. *Inorg. Chem.*, following paper in this issue.
(35) Mukherjee, R. N.; Abrahamson, A. J.; Patterson, G. S.; Stack, T. D. P.; Holm, R. H. *Inorg. Chem.* **1988**, *27*, 2137.

coordinate, and labile in both Fe(II) and Fe(III) complexes. Hemes are found with a variety of spin states and coordination numbers of 5 or 6 depending upon the field strength of the axial ligands.[36]

A second important factor in the FeN_4 system is its high reduction potential in comparison with that of the heme, Fe(salen), or bleomycin systems. Generally, the $dmgBF_2$ system is 500 mV more oxidizing than its heme or Fe(salen) analogue. In fact the $FeN_4(CH_3CN)_2^+$ species lies at a potential comparable to that of compound I of horse radish peroxidase.[37]

An unfortunate consequence of the strong oxidizing character of this system is that a number of axial ligated derivatives are too unstable toward spontaneous reduction to be easily detected. This includes all bis(amine) complexes as well as complexes containing CN^- or SR^-. In the less oxidizing Fe(salen), heme, or other systems slow spontaneous reduction by CN^-,[38] piperidine,[39] and SR^-[35] of Fe(III) to Fe(II) is reported. As a general rule, species with potentials above 0.7 V vs SCE containing oxidizable ligands were difficult to detect in visible or EPR spectroscopy. Lever[40] has described an empirical set of parameters which are an excellent guide to the redox potential of metal complexes in CH_3CN solution, and the relative stabilities of the ferric systems described here are consistent with these.

The low-spin character of FeN_4 is also manifested in the chemistry of the oxo-bridged diiron species. Heme, Fe(salen), and a variety of other oxo-bridged diiron complexes are 5-coordinate and display oxo to Fe charge-transfer bands in the 300–400-nm region. The $[FeN_4(L)]_2O$ systems are 6-coordinate and undergo ligand substitution trans to the oxo bridge in solution. From the reactions outlined in eqs 4 and 7, π-donor ligands lead to oxo-bridge cleavage, while π-acceptor ligands and good σ-donors tend to stabilize the oxo bridge. Detailed investigations of the effects of trans ligands on the reactions of the oxo-bridged complexes are in progress.

Acknowledgment. Support of the Natural Sciences and Engineering Research Council of Canada is gratefully acknowledged.

Registry No. $[FeN_4(CH_3CN)]_2O$, 136676-32-9; $[FeN_4(py)]_2O$, 136676-33-0; $[FeN_4(MeIm)]_2O$, 136676-34-1; $[FeN_4(TMIC)]_2O$, 136676-35-2; $Et_4N[FeN_4Cl_2]$, 136676-37-4; $Et_4N[FeN_4Br_2]$, 136676-39-6; $FeN_4(CH_3CN)_2^+$, 136676-40-9; $FeN_4(CH_3CN)_2^+PF_6^-$, 136676-41-0; $FeN_4(CH_3CN)_2^+ClO_4^-$, 136676-42-1; $[FeN_4(CH_3CN)_2^+]_2SO_4^{2-}$, 136676-43-2; $[FeN_4]_2O$, 136676-45-4; $FeN_4(SCN)_2^-$, 136676-44-3.

(36) Scheidt, W. R.; Reed, C. A. *Chem. Rev.* **1981**, *81*, 543.
(37) Hayashi, Y.; Yamazaki, I. *J. Biol. Chem.* **1979**, *254*, 9001.
(38) Del Gaudio, J. L.; La Mar, G. N. *J. Am. Chem. Soc.* **1976**, *98*, 3014.
(39) Del Gaudio, J.; La Mar, G. N. *J. Am. Chem. Soc.* **1978**, *100*, 1112.
(40) Lever, A. B. P. *Inorg. Chem.* **1990**, *29*, 1271.

Contribution from the Department of Chemistry,
York University, North York, Ontario, Canada M3J 1P3

Kinetics of the Reduction of Oxo-Bridged Diiron Complexes of Bis(difluoro(dimethylglyoximato)borate) with Hydroxy Aromatics, Amines, and Phosphines

Horst Noglik, David W. Thompson, and Dennis V. Stynes*

Received April 23, 1991

We present the first detailed study of rates of reduction of an oxo-bridged diiron complex with a variety of reducing agents including hydroquinones, catechols, substituted phenols, anilines, and phosphines. Overall results are consistent with coordination of the reductant trans to the oxo bridge via replacement of a labile CH_3CN followed by electron transfer and oxo-bridge cleavage. *N,N,N',N'*-tetramethyl-1,4-phenylenediamine (Wurster's reagent) reacts in a two-step reaction in which Wurster's blue is produced and then destroyed. The reactivity of the oxo-bridged complex is compared with that of the heme and Fe(salen) systems, and relationships to more active oxidants are discussed. The importance of the ligand environment in controlling activation of dioxygen by iron(II) in the catalyzed autoxidation of hydroquinone and peracid oxidation of 2,4,6-tri-*tert*-butylphenol is described.

Introduction

Oxo-bridged diiron complexes are well-known[1] and have been widely studied as models for a variety of non-heme iron proteins[2] known to possess this structural unit. Spectroscopic, magnetic, and structural investigations of the oxo-bridged diiron unit are extensive. However, few chemical reactions associated with Fe–O–Fe have been described, and no detailed studies of its redox reactions are reported. The "oxo dimer" is usually considered a chemical dead end in heme and Fe(salen) systems.

In a broader context the oxo-bridged diiron species is one of several potentially active oxidants accessible via dioxygen binding/O–O bond fission or via the so called "peroxide shunt" route[3] using peracids or iodosylbenzene as the oxidant in place of dioxygen. Scheme I summarizes the entry into these oxidants via dissociative substitution in Fe(II) complexes with two functional coordination sites. (L is a neutral monodentate ligand, and charges assume a dianionic N_4 ligand not shown.) The exact relationships among the several active oxidants listed in Scheme I are largely unknown,[5] and no information about the kinetics of substrate oxidations by them is available, even in widely studied heme models for P450 chemistry.[3] In a catalytic process where the active oxidant is only a transient intermediate, the task is elucidating the "active oxidant" is a formidable problem. In the few cases where kinetic data are available,[6,7] formation of the active oxidant

Scheme I. Dissociative Entry into Active Oxidants Using O_2 or XO (XO = Peracids, Amine Oxides, Iodosylbenzene, etc.)[4] and Inhibition by CO

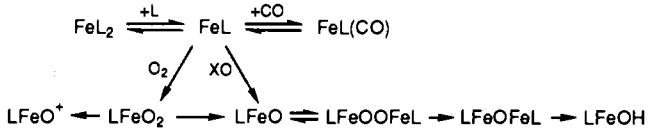

(1) Kurtz, D. M. *Chem. Rev.* **1990**, *90*, 585.
(2) Vincent, J. B.; Olivier-Lilley, G. L.; Averill, B. A. *Chem. Rev.* **1990**, *90*, 1447.
(3) (a) *Cytochrome P-450: Structure, Mechanism, and Biochemistry*; Ortiz de Montellano, P. R., Ed.; Plenum: New York, 1986. (b) White, R. E.; Coon, M. J. *Annu. Rev. Biochem.* **1980**, *49*, 315. (c) Guengerich, F. P.; MacDonald, T. L. *Acc. Chem. Res.* **1984**, *17*, 9. (d) Sheldon, R. A.; Kochi, J. K. *Metal Catalyzed Oxidations of Organic Compounds*; Academic Press: New York, 1981.
(4) If an Fe(III) complex is used instead of the initial Fe(II) shown above (as is the case in heme studies),[22] reaction with XO produces the $LFeO^+$ active oxidant.
(5) Balch, A. L.; Chan, Y.-W.; Cheng, R.-J.; LaMar, G. N.; Latos-Grazynski, L.; Renner, M. W. *J. Am. Chem. Soc.* **1984**, *106*, 7779.
(6) (a) Traylor, T. G.; Lee, W. A.; Stynes, D. V. *Tetrahedron* **1984**, *337*. (b) Traylor, T. G.; Lee, W. A.; Stynes, D. V. *J. Am. Chem. Soc.* **1984**, *104*, 755.

0020-1669/91/1330-4571$02.50/0